Supply Chain and Operations Decision Making

www.scodm.reapress.com

Sup. Chain Oper. Decis. Mak. Vol. 3, No. 1 (2026) 63–75.

Paper Type: Original Article

Designing a Blood Supply Chain Network: A Bi-Objective Robust Optimization Approach

Mohammadhasan Zarei[1,*], **Mohsen Varmazyar**[1]

[1] Industrial Engineering, Sharif University of Technology, Tehran, Iran; mh_zarei@ie.sharif.edu; varmazyar@sharif.edu.

Citation:

Received: 30 May 2025 *Revised: 27 July 2025* *Accepted: 29 September 2025*	Zarei, M., & Varmazyar, M. (2026). Designing a blood supply chain network: A bi-objective robust optimization approach. *Supply Chain and Operations decision making, 3*(1), 63-75.

Abstract

Managing blood supply chains and network design is challenging due to product perishability, uncertain supply and demand, and blood type compatibility. We present a two-stage robust optimization model for multi-product flows of red cells, platelets, and plasma, integrating strategic facility decisions with adaptive operational allocation under white, yellow, and red scenarios. An augmented ε-constraint method uncovers cost–time trade–offs, while robust optimization guards against extreme disruptions. In this study, we use real data from Tehran's blood transfusion organization and solve the model with CPLEX. We demonstrate that allowing substitutions compatible with the ABO blood group system and the Rhesus factor (ABO–Rh) relieves inventory pressure and reduces expected costs. The resulting Pareto frontier guides decision-makers in balancing delivery time against operating expenses.

Keywords: Blood supply chain, Robust optimization, Network design, ABO–Rh compatibility, Multi-objective optimization, Augmented ε-constraint.

1 | Introduction

The blood supply chain is a lifeline to modern health care systems, directly supporting and maximizing patient survival. Because an artificial substitute has not yet been developed, every unit of blood must be drawn by voluntary donation, tested, separated into red cells, platelets, and plasma, and refrigerated under strict temperature controls. Final products pass through a hierarchical system of fixed donor centers and mobile donor sites, regional blood banks, and specialized distribution centers to hospitals.

This network is very sensitive; blood components perish quickly, supply and demand fluctuate with seasons, donor drives, or random disasters, and each transfusion must satisfy ABO–Rh compatibility. Even in regular conditions, orchestrating shortage risk versus outdating requires constant strategic and operational planning. During emergencies such as the 2003 Bam earthquake, where only 23% of the 108 000 units contributed were used, or the COVID-19 outbreak that cut donations by as much as 30%, such issues are evident [1].

Corresponding Author: mh_zarei@ie.sharif.edu

https://doi.org/10.48313/scodm.v3i1.52

Earlier studies have addressed parts of the problem using deterministic cost minimization, two-stage stochastic programming, or robust optimization to mitigate extreme shocks. None of them, however, adopted multi-product flows, perishability, blood-type matching, and a multilayer network structure within a single integrated framework.

In this work, we first simulate a blood-layer network that includes collection sites, a central hub bank, regional banks, and end-user hospitals. A robust optimization method then places product-age limits and demand-supply variance under worst-case pandemic-like scenarios. The model pursues two objectives: minimum response time and total cost, and uses an enhanced ε-constraint approach to generate the Pareto frontier. Validation uses real-world data from the Tehran Blood Transfusion Organization.

The remainder of the paper is structured as follows. Section 2 discusses important research on blood chain modeling. Section 3 introduces the methodology and proposed robust, multi-product optimization. Section 4 gives Tehran data and numerical results, and Section 5 offers conclusions and recommendations for further research.

2 | Literature Review

At the beginning of the 2000, researchers relied on deterministic models with fixed demand, supply, and travel times. Katsaliaki [2] showed that simple inventory policies could deliver substantial savings. To better capture uncertainty, two-stage stochastic programming emerged. Najafi et al.'s chance-constrained formulation [3] reduced shortages, spoilage, and emergency transfers, while Xu and Szmerekovsky [4] decoupled strategic and operational decisions to improve resilience across demand scenarios. Zhang et al. [5] later used a Markov decision process for platelet allocation, cutting wastage by about 20 %.

Robust optimization was then adopted to protect against worst-case conditions. Ben Tal and Nemirovski [6] demonstrated that robust solutions sustain performance without sacrificing quality under data uncertainty. Building on this idea, Jabbarzadeh et al. [7] developed Iran's first disaster-ready blood network, and Hamdan and Diabat [8] utilized disruption scenarios and a Lagrangian approach to reduce worst-case delivery cost and time by up to 40 %. This paper serves as a base paper for the present research. Recent work has shifted toward hybrid, flexible formulations. Khalilpourazari and Hashemi Doulabi [9] introduced a fuzzy-interval-based robust model with chance constraints, and Tirkolaee et al. [10] applied possibilistic programming during the COVID-19 pandemic. For post-disaster relief, Entezari et al. [11] proposed a bi-objective stochastic routing model that reduced shortages by 53%, while Abdolazimi et al. [12] built a multi-objective, data-driven network using Benders decomposition for pandemic conditions.

While these advancements exist, the deficit lies in an integrated model that simultaneously covers all of the prominent products, platelets, red cells, and plasma, properly considers product age and perishability, is robust under pandemics or crises, and keeps total cost at a minimum in relation to response time. This deficit is addressed through our work by developing a two-objective, multi-product robust optimization model, validated with real data from the Tehran Blood Transfusion Organization.

3 | Methodology

In this section, we present our multi-objective blood supply chain and two-stage robust optimization model for Tehran's blood supply network, using an augmented ε-constraint to balance cost and delivery time under uncertainty.

3.1 | Overall Description

We develop a two-stage, multi-product optimization model for the blood supply chain in Tehran that encompasses the entire donor-to-patient process. The system is to be a four-tiered architecture: 1) a donation tier that combines mobile donations with fixed donation points, 2) a processing tier where whole blood is separated into red cells, platelets, and plasma, 3) a storage tier comprised of a single central hub bank and a

few regional banks, and 4) a demand tier comprising receiving hospitals. Stage one, strategic choices—pre-made before the appearance of any uncertainty—choose which permanent centers to open. Once an uncertainty scenario occurs, stage two, operating decisions, place the mobile facilities, truck raw blood, and components through the network, manage inventory stock across age classes, deliver orders to hospitals, and discard old units. The model concurrently minimizes overall cost (transport, holding, shortage and wastage, fixed cost) and network response time, trading off cost as the objective function against an extended ε-constraint for travel time to outline the Pareto frontier. Robust optimization techniques are incorporated to keep the solution viable under extreme supply and demand shocks such as earthquakes or pandemics. All parameters are normalized using simulation-based estimates from the Tehran Blood Transfusion Organization; thus, the resultant framework is always in contact with operational reality and ready to be tested in practice.

3.2 | Mathematical Model Formulation

In this section, we present the mathematical formulation of the problem under study.

3.2.1 | Notations

Sets:

I	Set of blood donors, indexed by i = 1, …, |I|
J	Set of temporary collection posts, indexed by j = 1, …, |J|
P	Set of permanent collection centres, indexed by p = 1, …,|P|
K	Set of all blood banks, indexed by k = 1, …, |K| $K^1 \in K$ central (hub) processing bank $K^2 \subseteq K$ set of regional (nonhub) banks
H	Set of hospitals, indexed by h = 1, …, |H|
B	Set of blood groups (O^+, O^-, …), indexed by b ∈ B
F	Set of blood components (red cells, platelets, plasma), indexed by f ∈ F
T	Set of planning periods, indexed by t
S	Set of uncertainty scenarios, indexed by s
A	Product age levels, indexed by a
E	Valid component age pairs {(f,a) | a ≤ L_f + 1}

Parameters:

DON_{ts}^{ib}	Maximum donors in region i with blood group b in period t under scenario s
DEH_{bts}^{hf}	Demand at hospital h for component f and blood group b in period t under scenario s
CPF_{ps}	Capacity of permanent collection centre p under scenario s
CMF_{js}	Capacity of mobile blood collection j under scenario s
CDF_{ks}	Direct donation capacity of Bank K under scenario s
STB_k	Total storage capacity of Bank K
FCP_p	Fixed cost to open or activate the center p
FCM_j	Fixed cost to set up mobile blood collection j

CJM_{ij}	Transport cost per whole blood bag from donor i to mobile blood collection j
CPP_{ip}	Transport cost per whole blood bag from donor i to center p
CKD_{ik}	Direct transport cost per bag from donor i to bank k
CPD_{pk^1}	Transport cost per bag from the center p to the central bank k^1
CJD_{jk^1}	Transport cost per bag from mobile blood collection j to central bank k^1
$CXD_{k^2k^1}$	Transport cost per whole blood bag from nonhub bank k^2 to central bank k^1
$CDX_{fk^2}^{k^1}$	Transport cost per product f from central bank k^1 to nonhub bank k^2
CKH_{fh}^{k}	Transport cost per product f from bank k to hospital h
TJM_{ij}	Travel time from donor i to mobile blood collection j
TPP_{ip}	Travel time from donor i to center p
TKD_{ik}	Travel time from donor i to bank k
TPD_{pk^1}	Travel time from the center p to the central bank k^1
TJD_{jk^1}	Travel time from mobile blood collection j to central bank k^1
$TXD_{k^2k^1}$	Travel time from nonhub bank k^2 to central bank k^1
$TDX_{fk^2}^{k^1}$	Travel time for product f from k^1 to k^2
TKH_{fh}^{k}	Transport cost per product f from bank k to hospital h
CHP_f	Holding cost per unit of product f per period
CSP_f	Shortage cost per unit of product f at the hospital
CWP_f	Waste cost per unit of product f after expiration
$MAT_{b_p}^{b_d}$	Compatibility matrix entry (1 if donor group b_p can serve demand b_d)
$PNL_{b_p}^{b_d}$	Penalty for using an incompatible donor group b_p for demand b_d
L_f	Shelf life of product f
$\alpha_{k^1}^{f}$	Conversion rate from whole blood to product f at central bank k^1
P_s	Probability of scenario s
n	The maximum number of centers that can be opened
N	Maximum number of active facilities for donors
M	Big-M

Decision variables:

x_p	1 if permanent collection center p is opened, 0 otherwise.
z_{ts}^{j}	1 if mobile blood collection j is active in period t under scenario s, 0 otherwise.
ap_{ts}^{ip}	1 if whole-blood allocation from donor i to center p is used in period t, scenario s, 0 otherwise.

aj_{ts}^{ij}	1 if whole-blood allocation from donor i to mobile blood collection j is used in period t, scenario s, 0 otherwise.
ak_{ts}^{ik}	1 if whole-blood allocation from donor i to bank k is used in period t, scenario s, 0 otherwise.
$pc_{ts}^{pk^1}$	1 if allocation from center p to hub bank k^1 is used in period t, scenario s, 0 otherwise.
$jc_{ts}^{jk^1}$	1 if allocation from mobile blood collection j to hub bank k^1 is used in period t, scenario s, 0 otherwise.
$cl_{ts}^{k^2k^1}$	1 if allocation from bank k^2 to central bank k^1 is used in period t, scenario s, 0 otherwise.
kh_{ts}^{kh}	1 if allocation from bank k to hospital h is used in period t, scenario s, 0 otherwise.
qp_{bts}^{ip}	Units of whole blood of group *b* from donor *i* to centre *p* in period *t*, scenario *s*
qj_{bts}^{ij}	Units of whole blood of group b from donor i to mobile blood collection j in period t, scenario s.
qk_{bts}^{ik}	Units of whole blood of group b from donor i to bank k in period t, scenario s.
$qc_{bts}^{pk^1}$	Units of whole blood of group b from centre p to hub bank k^1 in period t, scenario s.
$qm_{bts}^{jk^1}$	Units of whole blood of group b from post j to hub bank k^1 in period t, scenario s.
$ql_{bts}^{k^2k^1}$	Units of whole blood of group b from regional bank k^2 to hub bank k^1 in period t, scenario s.
$qb_{bats}^{k^1k^2f}$	Units of component f (group b, age a) sent from hub bank k^1 to regional bank k^2 in period t, scenario s.
$qh_{b_pats}^{khfb_d}$	Units of component f (donor group b_p, age a) sent from bank k to hospital h for demand group b_d in period t, scenario s.
i_{ats}^{kfb}	Inventory of component f, group b, age a at bank k at end of period t, scenario s.
w_{ats}^{kfb}	Wasted units of component f, group b, at age $a=L_f+1$ at bank k in period t, scenario s.
sh_{ats}^{hfb}	Shortage of component f, group b at hospital h in period t, scenario s.

Objective functions:

$$\begin{aligned}\min f1 \;=\; & \sum_{p} FCP_p\, x_p + \sum_{j,t,s} FCM_j\, z_{ts}^{j} \\ & + \sum_{i,b,t,s}\Big(\sum_{p} CPP_{ip}\, qp_{bts}^{ip} + \sum_{j} CJM_{ij}\, qj_{bts}^{ij} + \sum_{k} CKD_{ik} qk_{bts}^{ik}\Big) \\ & + \sum_{k^1,t,s}\Big(\sum_{p,b} CPD_{pk^1}\, qc_{bts}^{pk^1} + \sum_{j,b} CJD_{jk^1}\, qm_{bts}^{jk^1} + \sum_{k^2,b} CXD_{k^2k^1} ql_{bts}^{k^2k^1}\Big) \\ & + \sum_{t,s}\Big(\sum_{e,k,b} CDX_{K^1fK^2}\, qb_{bats}^{k^1k^2f} + \sum_{r,k,h,b} CKH_{kfh}\, qh_{b_pats}^{khfb_d}\Big) \\ & + \sum_{t,s}\Big(\sum_{k,f,b,a} CHP_f\, i_{ats}^{kfb} + \sum_{h,f,b} CSH_f\, sh_{bts}^{hf} + \sum_{k,f,b} CWP_f w_{(L_f+1)ts}^{kfb}\Big) \\ & + \sum_{e,k,b,h,t,s} (PNL_{b_p}^{b_d} + L_f - (a-1)) qh_{b_pats}^{khfb_d}.\end{aligned} \tag{1}$$

$$\min f2 = \sum_{t,s}\Big(\sum_{i,p,b} TPP_{ip}\, qp_{bts}^{ip} + \sum_{j,j,b} TJM_{ij}\, qj_{bts}^{ij} + \sum_{i,k,b} TKD_{ik} qk_{bts}^{ik}\Big)$$

$$+ \sum_{k^1,t,s}\Big(\sum_{p,b} TPD_{pk^1}\, qc_{bts}^{pk^1} + \sum_{j,b} TJD_{jk^1}\, qm_{bts}^{jk^1} + \sum_{k^2,b} TXD_{k^2k^1} ql_{bts}^{k^2k^1}\Big) \quad (2)$$

$$+ \sum_{k,f,b,a,t,s} TDX_{K^1fK^2}\, qb_{bats}^{k^1k^2f} + \sum_{k,f,b,a,t,s} TKH_{fh}^{k}\, qb_{b_pats}^{khfb_d}.$$

The first objective, F_1, consolidates all cost components of the blood supply network into a single expression: it sums the fixed opening costs of mobile and temporary collection centres; the transportation costs of whole blood from donors to permanent centres, mobiles, and banks the shipping costs of processed components to the central hub (k^1) and onward to regional banks (k^2); the delivery costs from banks to hospitals; and finally the combined inventory holding, shortage penalty, waste costs, and penalties for blood group matches or near expiry units.

The second objective, F_2, captures the system's total transport time: it aggregates the travel times for moving whole blood from donors to all collection points and banks, the transit of processed components from the hub k1 to each regional bank k^2, and the final distribution to hospitals. Minimizing F_2 thus optimizes both network design and routing to reduce delivery times for blood and its products.

Constraints:

$$\sum_{p} x_p \le n. \quad (3)$$

$$\sum_{j} z_{ts}^{j} \le N - n, \qquad \forall\, t, s. \quad (4)$$

$$ap_{ts}^{ip} \le x_p, \qquad \forall\, i, p, t, s. \quad (5)$$

$$aj_{ts}^{ij} \le z_{ts}^{j}, \qquad \forall\, i, j, t, s. \quad (6)$$

$$\sum_{j} aj_{ts}^{ij} + \sum_{p} ap_{ts}^{ip} + \sum_{k} ak_{ts}^{ik} \le 1, \qquad \forall\, i, t, s. \quad (7)$$

$$pc_{ts}^{pk^1} \le x_p, \qquad \forall\, p, t, s. \quad (8)$$

$$jc_{ts}^{jk^1} \le z_{ts}^{j}, \qquad \forall\, j, t, s. \quad (9)$$

$$\sum_{k} kh_{ts}^{kh} \le 1, \qquad \forall\, h, t, s. \quad (10)$$

$$\sum_{i,b} qp_{bts}^{ip} \le CPF_{ps} x_p, \qquad \forall\, p, t, s. \quad (11)$$

$$\sum_{i,b} qj_{bts}^{ij} \le CMF_{js} z_{ts}^{j}, \qquad \forall\, j, t, s. \quad (12)$$

$$\sum_{i,b} qk_{bts}^{ik} \le CDF_{ks}, \qquad \forall\, k, t, s. \quad (13)$$

$$qj_{bts}^{ij} \le DON_{ts}^{ib} aj_{ts}^{ij}, \qquad \forall i, j, b, t, s. \quad (14)$$

$$qp_{bts}^{ip} \le DON_{ts}^{ib} ap_{ts}^{ip}, \qquad \forall i, p, b, t, s. \tag{15}$$

$$qk_{bts}^{ik} \le DON_{ts}^{ib} ak_{ts}^{ip}, \qquad \forall i, k, b, t, s, \tag{16}$$

$$qc_{bts}^{pk^1} \le M\, pc_{ts}^{pk^1}, \qquad \forall i, k^1, b, t, s. \tag{17}$$

$$qm_{bts}^{jk^1} \le Mjc_{ts}^{jk^1}, \qquad \forall j, k^1, b, t, s. \tag{18}$$

$$qh_{b_p ats}^{khfb_d} \le M\, kh_{ts}^{kh}, \qquad \forall k, h, f, b_d, b_p, a, t, s. \tag{19}$$

$$\sum_{i} qp_{bts}^{ip} = qc_{bts}^{pk^1}, \qquad \forall p, b, k^1, t, s. \tag{20}$$

$$\sum_{i} qj_{bts}^{ij} = qm_{bts}^{jk^1}, \qquad \forall j, b, k^1, t, s. \tag{21}$$

$$ql_{bts}^{k^2k^1} \le M\, cl_{ts}^{k^2k^1}, \qquad \forall b, k^1, k^2, t, s. \tag{22}$$

$$\sum_{i} qk_{bts}^{ik} = ql_{bts}^{k^2k^1}, \qquad \forall k^1, k^2, b, t, s. \tag{23}$$

$$\sum_{f,b,a} i_{ats}^{kfb} \le STB_k, \qquad \forall k, t, s. \tag{24}$$

$$WB_{bts}^{k^1} = \sum_{j} qm_{bts}^{jk^1} + \sum_{p} qc_{bts}^{pk^1} + \sum_{k^2} ql_{bts}^{k^2k^1} + \sum_{k^1} qk_{bts}^{ik^1},$$

$$IN_{k^1ts}^{fb} = \alpha_f\, WB_{bts}^{k^1},$$

$$OUT_{k^1ts}^{fb} = \sum_{h,b_d} qh_{b_p ats}^{k^1 hfb_d} + \sum_{k^2} qb_{bats}^{k^1k^2f}.$$

$$\sum_{a=1}^{L_f} i_{ats}^{k^1fb} + w_{(L_f+1)ts}^{k^1fb} = \sum_{t=1}^{T} IN_{ts}^{fb} - \sum_{a,t} OUT_{k^1ts}^{fba}, \qquad \forall k^1, f, b, t, s. \tag{25}$$

$$IN_{k^2ts}^{fb} = qb_{bats}^{k^1k^2f},$$

$$OUT_{K^2ts}^{fba} = \sum_{h,b_d} qh_{b_p ats}^{k^2 hfb_d}.$$

$$\sum_{a=1}^{L_f} i_{ats}^{k^2fb} + w_{(L_f+1)ts}^{k^2fb} = \sum_{t=1}^{T} IN_{k^2ts}^{fb} - \sum_{a,t} OUT_{k^2ts}^{fba}, \forall k^2, f, b, t, s. \tag{26}$$

$$w_{bts}^{kf} = \sum_{a=1}^{L_f} i_{a(t-1)s}^{kfb}, \qquad \forall k, f, b, t, s. \tag{27}$$

$$\sum_{b_p,a} qh_{b_p ats}^{kfb_d} \le \sum_{b_p,a} i_{ats}^{kfb_p}, \qquad \forall k, h, b_d, t, s. \tag{28}$$

$$\sum_{k^2,a} qb_{bats}^{k^1k^2f} \le \sum_{b_p,a} i_{ats}^{kfb_p}, \qquad \forall\, k^1, f, t, s. \tag{29}$$

$$\sum_{k,b_p,a} qh_{b_pats}^{kfb_d} + sh_{bts}^{hf} = DEH_{ts}^{hfb_d}, \quad \forall\, h, f, b_d, t, s. \tag{30}$$

$$x_p, z_{ts}^{j}, ap_{ts}^{ip}, aj_{ts}^{ij}, ak_{ts}^{ik}, pc_{ts}^{pk^1}, jc_{ts}^{jk^1}, cl_{ts}^{k^2k^1}, kh_{ts}^{kh} \in \{0,1\}, \qquad \forall\, i, p, j, k, h, t, s. \tag{31}$$

$$qp_{bts}^{ip}, qj_{bts}^{ij}, qk_{bts}^{ik}, qc_{bts}^{pk^1}, qm_{bts}^{jk^1}, ql_{bts}^{k^2k^1}, qb_{bats}^{k^1k^2f},$$

$$qh_{b_pats}^{khfb_d}, i_{ats}^{kfb}, w_{ats}^{kfb}, sh_{ats}^{hfb} \ge 0\ , \forall\, i, j, p, k, h, b, a, t, s. \tag{32}$$

Constraints (3)–(11) specify the basic network topology and the admissible shipment routes for each period and scenario. They require that at most n fixed collection posts are open and at most N–n mobile posts are in use, that any donor donates blood down at most one open outward path, that center or post deliveries to the central hub bank occur only if the nodes are open, and that each hospital be served by exactly one bank. They also restrict the inflow of whole blood to set centers, mobiles, and direct transfers from banks by their capacities. *Constraints (12)–(16)* connect inbound flows to the actual number of available donors or the activation status of each path, preventing any flow that lacks donor supply or is not permitted by the path. With Big-M logic, *Constraints (17)–(19)* also prohibit outbound shipments from centers, posts, or banks to hospitals except when the relevant binary "allocation" variable is activated. Flow balance *constraints (20)* and *(21)* require the input and output totals to agree exactly at all fixed centers and mobile posts. *Constraints (22)* and *(23)* do the same for deliveries to and from the central node to and between region banks, and *Constraint (24)* forces the total capacity in each bank. Inventory and waste balances in the hub and regional banks are imposed by *Constraints (25)* and *(26)*, which balance incoming, outgoing, and expired units; Constraint (27) balances any end-of-period stock that becomes waste in the next period. *Constraints (28)* and *(29)* prevent shipping more units than currently in inventory to hospitals or between banks. *Constraint (30)* ensures that the demand for each blood product at hospitals is satisfied through supplied units and allowable shortage levels across all periods and scenarios.

Finally, *Constraints (31)* and *(32)* are constraints on the sign of the variables.

3.3 | Conversion to a Single-Objective Model

To formulate the bi-objective model into a single objective and identify the Pareto frontier, we apply the augmented ε-constraint approach. The F_1 cost function is used as the main objective, and the delivery time function of F_2 is used as a constraint with an upper limit ε as the delivery time tolerance. It implies that the initial two-objective formulation is reduced to the following:

$$\min_x F_1(x) + \delta \frac{S_1}{r_1},$$

s.t.

$$F_2(x) + S_1 = \epsilon.$$

$$Constraints\ (3) - (31). \tag{32}$$

3.4 | Robust Model

Aghezzaf et al. [13] suggest a robust optimization approach that incorporates a deterministic model into a two-stage stochastic program. Let S = {1, ⋯, |S|} be the set of scenarios with probabilities p_s. One would like to determine decisions $x \in X$ that are good on average and under worst-case conditions by solving:

$$\min_x \mu \max_s(\xi_s - \xi_s^*) + \lambda \sum_s P_s \xi_s,$$
$$\text{s.t.} \quad x \in X. \tag{33}$$

Here, ξ_s^* is the optimal cost when situations occur in the deterministic model, and ξ_s is the actual cost when s is encountered. The parameters μ and λ balance worst-case robustness (μ large) against expected value (λ large).

In the *Eq. (33)*, ξ_s represents the value of the first objective function.

The objective *function (33)* can be linearized by letting $Q = \max_s(\xi_s - \xi_s^*)$ and, incorporating the constraints

$$Q \geq \xi_s - \xi_s^*, \qquad \forall s \in S.$$

This results in the following optimized formulation:

$$\beta = \min \mu . Q + \lambda . \sum_s P_s \xi_s,$$
$$Q \geq \xi_s - \xi_s^*, \qquad \forall s \in S.$$
$$\text{s.t.} \tag{34}$$
$$(3) - (32).$$

Finally, we have the final model:

$$\min \beta + \delta \frac{S_1}{r_1},$$
$$\text{s.t.}$$
$$F_2(x) + S_1 = \epsilon,$$
$$Q \geq \xi_s - \xi_s^*, \qquad \forall s \in S,$$
$$Constraints\ (3) - (31). \tag{35}$$

3.5 | Demand Distribution

To evaluate the performance and robustness of our proposed model under various scenarios, we developed a synthetic dataset that best captures the statistical behavior of true demand observations. This argument was accomplished in two main steps: 1) identifying the best fit distribution: we used various families of distributions (e.g., Normal, Lognormal, etc.) with the Python Fitter library to fit the empirical data and selected the best goodness of fit, and 2) generation of synthetic data: we generated the sample from the selected distribution using its estimated parameter to create the simulation dataset. To assess whether the synthetic data fit the empirical pattern, we used the Kolmogorov–Smirnov test. The test calculates the statistic D as the supremum of the absolute difference between the empirical and theoretical cumulative distribution functions and provides the corresponding p-value.

$$D = \sup_{x} \left| F_{emprical}(x) - F_{theroretical}(x) \right|. \quad (36)$$

I. Null hypothesis (H_0): the data follow the selected distribution.

II. Alternative hypothesis (H_1): the data do not follow the selected distribution.

We set the significance level to $\alpha = 0.05$. If the p-value $\geq \alpha$, we do not reject H_0 and the distribution is deemed acceptable for simulation; otherwise, we reject H_0 and exclude that distribution.

Table 1. Distribution fitting results.

S	Prod.	Dist.	Params.	P-V
S_1	F_1	Normal	μ = 975.49, σ = 249.02	0.9342
S_1	F_2	3-component Normal mixture	w = [0.525, 0.205, 0.270], μ = [1487.03, 611.25, 2708.49], σ = [317.10, 167.12, 621.98]	0.8834
S_1	F_3	2-component Normal mixture	w = [0.404, 0.596], μ = [441.45, 899.91], σ = [181.61, 209.02]	0.8164
S_2	F_1	Burr Type XII	c = 7.440, d = 2.482, loc = 0.058, scale = 1158.24	0.9914
S_2	F_2	3-component Normal mixture	w = [0.503, 0.205, 0.292], μ = [2208.15, 1620.22, 826.78], σ = [243.54, 251.74, 256.29]	0.8143
S_2	F_3	3-component Normal mixture	w = [0.294, 0.506, 0.199], μ = [967.97, 739.79, 328.70], σ = [160.17, 120.29, 71.60]	0.9903
S_3	F_1	Normal	μ = 983.07, σ = 167.92	0.9697
S_3	F_2	Relativistic Birnbaum–Saunders	ϱ = 2.8929, loc = 407.00, scale = 441.06	0.9207
S_3	F_3	3-component Normal mixture	w = [0.2107, 0.4922, 0.2970], μ = [363.70, 791.70, 1001.19], σ = [86.25, 126.57, 118.86]	0.9675

4 | Data Overview and Numerical Results

In this section, we first describe the Tehran case study and data sources, then outline the implementation setup, and finally present key numerical results and Pareto analyses to demonstrate the model's performance.

4.1 | Case Study

To validate our model, we conducted a case study of the blood supply chain in Tehran. The city has 22 regions and six permanent blood donation sites. Additionally, 13 other regions were considered potential locations for temporary donation booths. The network comprises four blood banks:

Vasal Blood Bank is the central bank, and three regional banks serve storage and hospital delivery. The latter three are also capable of direct collection. We selected 25 hospitals, one from each region except Region 6, as local demand nodes. Donor-center capacities were obtained from the Iran Blood Transfusion Organization's bed statistics, and transport distances and costs were estimated using Google Maps data. Throughout this case study, we did our best to replicate real - life circumstances as closely as possible. The model's structure and parameters were thus perfectly fitted to Tehran's current blood supply system.

4.2 | Implementation and Results

The model was implemented in Python using the Pyomo library and solved with the CPLEX optimizer on a laptop with an Intel Core i7-13650HX processor and 32 GB RAM. Two configurations were tested: the first, where blood group substitution is performed according to ABO–Rh compatibility rules, and the second, where any substitution is not allowed. The numerical result is shown with the Pareto frontier plot.

Table 2. Results for $\mu = 0.25$, $\lambda = 0.75$ without Compatibility.

ϵ	F_1	F_2	Time(s)
0	$7.13*10^9$	0	3.94
208629	$6.32*10^9$	208530	12.8
417259	$6.32*10^9$	417213.9	54.49
625888	$6.32*10^9$	625752.9	62.99
834517	$6.32*10^9$	834491.2	233.71
1043147	$6.32*10^9$	1042955	74.77
1251776	$6.32*10^9$	121711	316.44

Table 3. Results for μ=0.25, λ=0.75 with Compatibility.

ϵ	F_1	F_2	Time(s)
0	$7.13*10^9$	0	9.94
302624	$6.03*10^9$	302621.5	85.29
605248	$5.29*10^9$	605233.8	350.41
907871	$4.65*10^9$	907865.7	1535.65
1210495	$4.15*10^9$	1205586	1880.7
1513119	$3.69*10^9$	1513093	2097.89
1815743	$3.05*10^9$	1815734	3841.51

To assess model behavior, we tried three values for μ: 0.25, 0.50, and 0.75, with λ set accordingly (e.g., μ= 0.25, λ =0.75). We measured the solution output and solve time for each value. Our results show that increasing λ reliably decreases the expected cost F_1. Furthermore, permitting blood group substitution based on ABO–Rh compatibility results in lower total costs than the no-substitution case. Such flexibility in inventory management reduces extreme inventory shortages and lowers shortage and waste penalties. Although it creates additional transportation routes, thus increasing F_2 travel times and distances, it is sufficiently offset by more intelligent routing and faster fulfillment of demand, resulting in a reduced system cost.

Pareto plots also show that when λ is large and cost is low, the curves shift down, as in *Figs. 1* and *2*. The plots easily demonstrate that by selecting a set of weight parameters, a decision maker can choose the optimal trade-off between delivery time and operating cost.

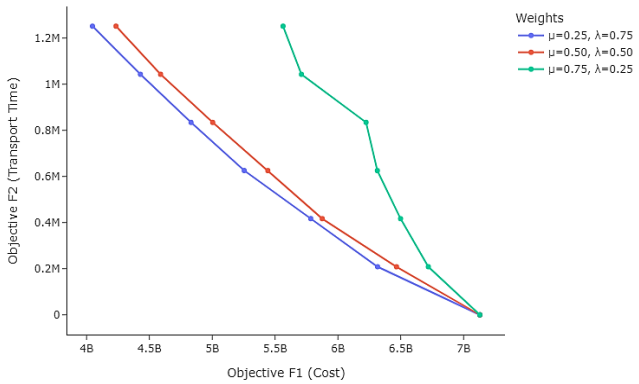

Fig. 1. Pareto-frontier without considering blood group compatibility.

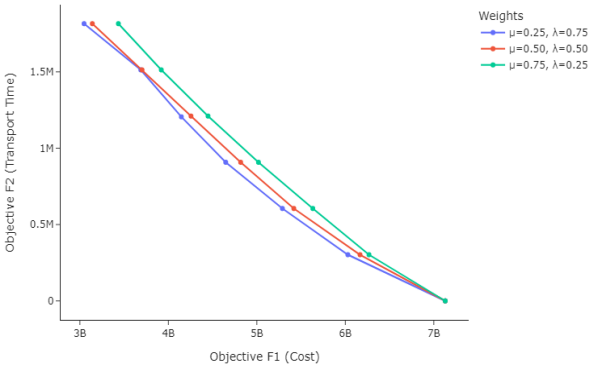

Fig. 2. Pareto-frontier considering blood group compatibility.

5 | Conclusion

We proposed a robust, bi-objective multi-product model for Tehran's blood supply chain network that explicitly handles perishability, blood group compatibility, and both fixed and mobile donation sites. Using an augmented ε-constraint approach, we minimized system cost and delivery time while mapping the Pareto trade-off and demonstrating solution stability under extreme demand and supply shocks. Our case study shows that blood group substitution reduces costs at the expense of slightly longer delivery times, and adjusting robustness weights allows decision-makers to balance cost and time. Future work could include dynamic donor behavior, real-time inventory tracking, stochastic travel times, and hybrid forecasting methods to scale the model to larger networks and to validate it in operational blood services.

Funding

This work was carried out without financial support from any public, commercial, or non-profit organizations.

Data Availability

The data are available from the corresponding author upon reasonable request.

Conflict of Interest

There are no competing interests to declare.

Consent for Publication

The authors confirm consent for the publication of this work.

References

[1] Sun, H., Li, J., Wang, T., & Xue, Y. (2022). A novel scenario-based robust bi-objective optimization model for humanitarian logistics network under risk of disruptions. *Transportation research part e: Logistics and transportation review*, *157*, 102578. https://doi.org/10.1016/j.tre.2021.102578

[2] Katsaliaki, K. (2008). Cost-effective practices in the blood service sector. *Health policy*, *86*(2), 276–287. https://doi.org/10.1016/j.healthpol.2007.11.004

[3] Najafi, M., Ahmadi, A., & Zolfagharinia, H. (2017). Blood inventory management in hospitals: Considering supply and demand uncertainty and blood transshipment possibility. *Operations research for health care*, *15*, 43–56. https://doi.org/10.1016/j.orhc.2017.08.006

[4] Xu, Y., & Szmerekovsky, J. (2022). A multi-product multi-period stochastic model for a blood supply chain considering blood substitution and demand uncertainty. *Health care management science*, *25*(3), 441–459. https://doi.org/10.1007/s10729-022-09593-5

[5] Zhang, C., Ayer, T., White, C. C., Bodeker, J. N., & Roback, J. D. (2023). Inventory sharing for perishable products: Application to platelet inventory management in hospital blood banks. *Operations research*, *71*(5), 1756–1776. https://doi.org/10.1287/opre.2022.2410

[6] Ben-Tal, A., & Nemirovski, A. (2000). Robust solutions of linear programming problems contaminated with uncertain data. *Mathematical programming*, *88*(3), 411–424. https://doi.org/10.1007/PL00011380

[7] Jabbarzadeh, A., Fahimnia, B., & Seuring, S. (2014). Dynamic supply chain network design for the supply of blood in disasters: A robust model with real world application. *Transportation research part e: Logistics and transportation review*, *70*, 225–244. https://doi.org/10.1016/j.tre.2014.06.003

[8] Hamdan, B., & Diabat, A. (2020). Robust design of blood supply chains under risk of disruptions using Lagrangian relaxation. *Transportation research part e: Logistics and transportation review*, *134*, 101764. https://doi.org/10.1016/j.tre.2019.08.005

[9] Khalilpourazari, S., & Hashemi Doulabi, H. (2023). A flexible robust model for blood supply chain network design problem. *Annals of operations research*, *328*(1), 701–726. https://doi.org/10.1007/s10479-022-04673-9

[10] Tirkolaee, E. B., Golpîra, H., Javanmardan, A., & Maihami, R. (2023). A socio-economic optimization model for blood supply chain network design during the COVID-19 pandemic: An interactive possibilistic programming approach for a real case study. *Socio-economic planning sciences*, *85*, 101439. https://doi.org/10.1016/j.seps.2022.101439

[11] Entezari, S., Abdolazimi, O., Fakhrzad, M. B., Shishebori, D., & Ma, J. (2024). A bi-objective stochastic blood type supply chain configuration and optimization considering time-dependent routing in post-disaster relief logistics. *Computers & industrial engineering*, *188*, 109899. https://doi.org/10.1016/j.cie.2024.109899

[12] Abdolazimi, O., Pishvaee, M. S., Shafiee, M., Shishebori, D., Ma, J., & Entezari, S. (2025). Blood supply chain configuration and optimization under the COVID-19 using benders decomposition based heuristic algorithm. *International journal of production research*, *63*(2), 571–593. https://doi.org/10.1080/00207543.2023.2263088

[13] Aghezzaf, E. H., Sitompul, C., & Najid, N. M. (2010). Models for robust tactical planning in multi-stage production systems with uncertain demands. *Computers & operations research*, *37*(5), 880–889. https://doi.org/10.1016/j.cor.2009.03.012